# Supplemental information

# Dopamine depletion selectively disrupts

# interactions between striatal neuron

# subtypes and LFP oscillations

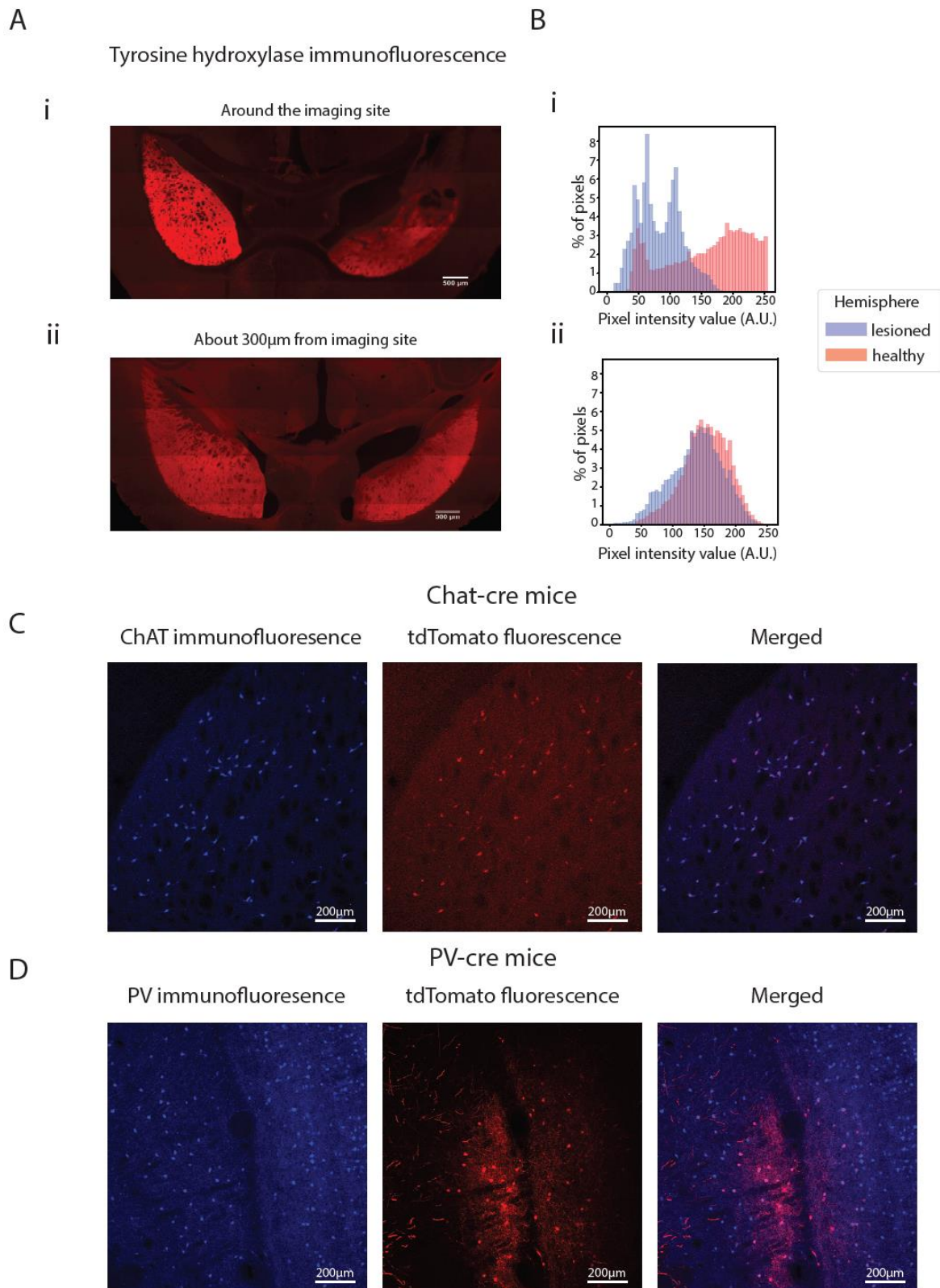**Dana Zemel, Howard Gritton, Cyrus Cheung, Sneha Shankar, Mark Kramer, and Xue Han**

**Figure S1. Histological quantification. Related to Figure 1 and Methods**
**(A)** Tyrosine hydroxylase (TH) immunofluorescence in an example horizontal slice across the dorsal striatum adjacent to the imaging window (**i**), and at ~300μm below the imaging window (**ii**). **(B)** Histogram of pixel fluorescence intensity in the striatal area corresponding to the lesioned (blue) and the healthy (pink) hemispheres. There was a reduction of TH immunofluorescence intensity of 17-63% near the imaging site across individual mice (20±21%, mean ± standard deviation, n=48 slices in 14 mice). **(C)** Choline acetyltransferase (ChAT) immunofluorescence (left), tdTomato fluorescence from labelled CHIs (middle), and merge (right) in an example Chat-cre mouse striatal brain slice. **(D)** Parvalbumin (PV) immunofluorescence (left), tdTomato fluorescence (middle) and merge (right) in an example PV-cre mouse striatal brain slice.
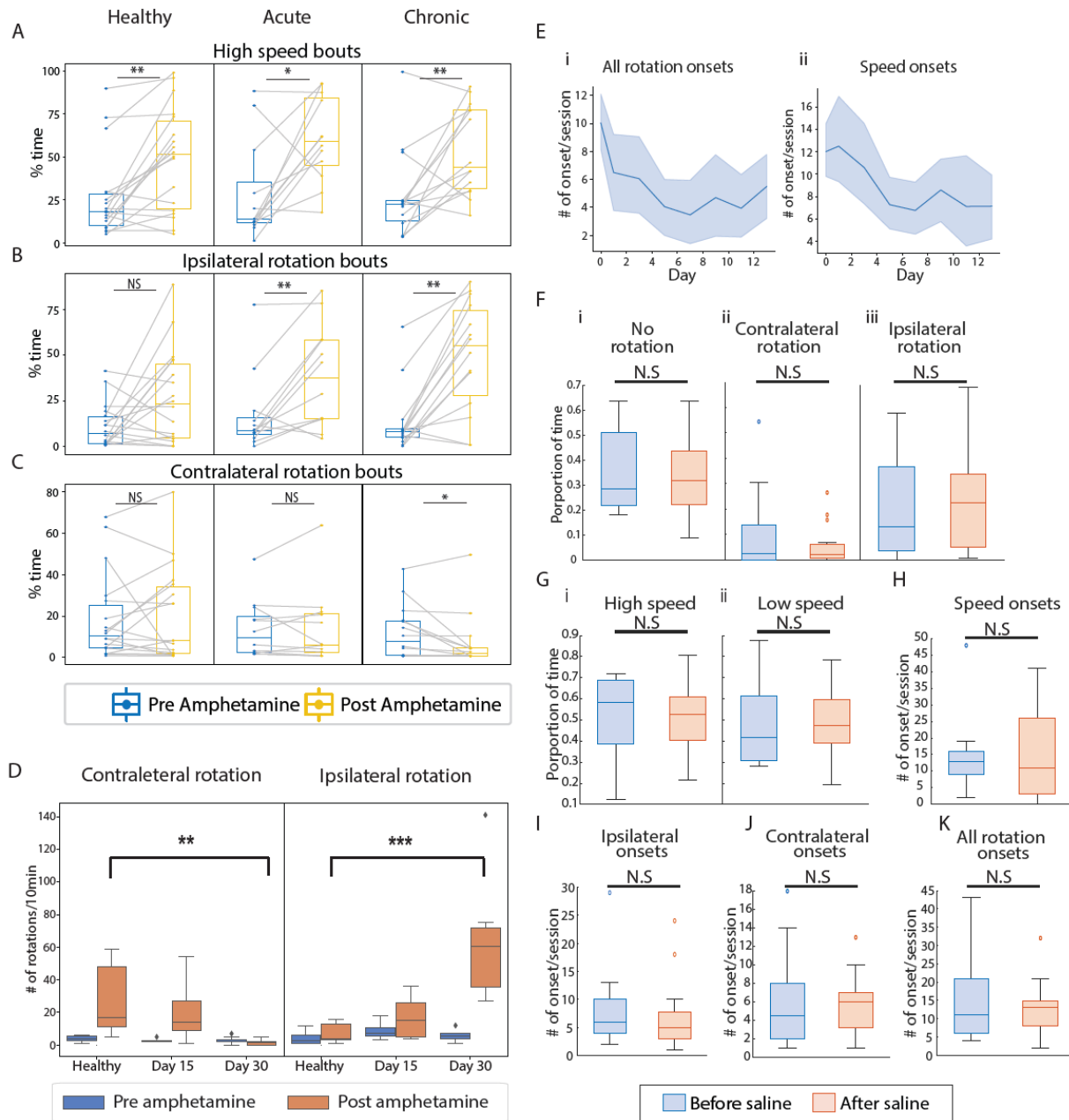
**Figure S2. Behavioral quantification upon 6-OHDA, saline, and amphetamine administration. Related to Figure 2.**
**(A-C)** Amphetamine induced behavioral changes analyzed on the spherical treadmill while head fixed. The fraction of time mice spent in high-speed bouts **(A)**, ipsilateral rotation bouts **(B)**, and contralateral rotation bouts **(C)**, before (blue) and after (yellow) amphetamine injection, before 6-OHDA injury (left), and on days 15 (middle) and 30 (right) after 6-OHDA injury. (Wilcoxon signed rank. High-speed bouts, post- vs. pre-amphetamine: Healthy: P= 0.003; Acute =0.016; Chronic: P=0.009. Ipsilateral rotation bouts post- vs. pre-amphetamine: Healthy: P=0.17; Acute: P=0.009; Chronic: P=0.001. Contralateral rotation bouts post- vs. pre-amphetamine: Healthy: P=0.83; Acute: P=0.97; Chronic: P=0.025.) **(D)** Amphetamine induced behavioral changes analyzed in open field. The number of contralateral (left) and ipsilateral (right) rotations, before (blue) and after (orange) amphetamine injection, before 6-OHDA injury, and on days 15 and 30 after 6-OHDA injury (ANOVA for interaction of ipsilateral rotation and conditions: $F(2,18)=32.68$, P= 0.001. Mixed-effect model: Acute vs. Healthy: t=2.255, P=0.075; Chronic vs. Healthy: t=8.059, P=2.78x10$^{-4}$; Contralateral rotations and conditions: $F(2,18) = 7.83$, P= 0.011. Mixed-effect model: Acute vs. Healthy: t=-1.252, P=0.250; Chronic vs. Healthy: t=-3.933 P=0.002). **(E)** Number of speed onsets (i) and rotation onsets (**ii**) during 10 minutes recording sessions over the two week period after 6-OHDA injection. **(F)** The proportion of time animals spent in no rotation (**i**), contralateral rotation (**ii**), and ipsilateral rotation bouts (**iii**), across sessions recorded before saline infusion (blue), and 3-10 days after saline infusion (orange) (n=9 mice). No significant differences between sessions before versus after saline infusion (t-test. No rotation: t(31)=0.052, P=0.959; contralateral rotation: t(31)=-0.458, p=0.65; ipsilateral rotation: t(31)=1.364, p=0.183.) **(G)** The proportion of time animals spent in high-speed bouts (**i**) and low-speed bouts (**ii**) across sessions before (blue) and after (orange) saline infusion. No significant differences were detected (t-test. high-speed: t(31)=0.056, p=0.956; low-speed: t(31)=-0.056, p=0.956.) **(H-K)** number of speed **(H)**, ipsilateral **(I)**, contralateral **(J)**, and all rotational **(K)** onsets, across sessions before (blue) and after (orange) saline infusion. No significant differences were detected (t-test. speed: t(31)=-0.157, p=0.876; ipsilateral: t(31)=0.233, p=0.817; contralateral: t(31)=0.439, p=0.664; all rotation: t(31)=0.425, p=0.674.)
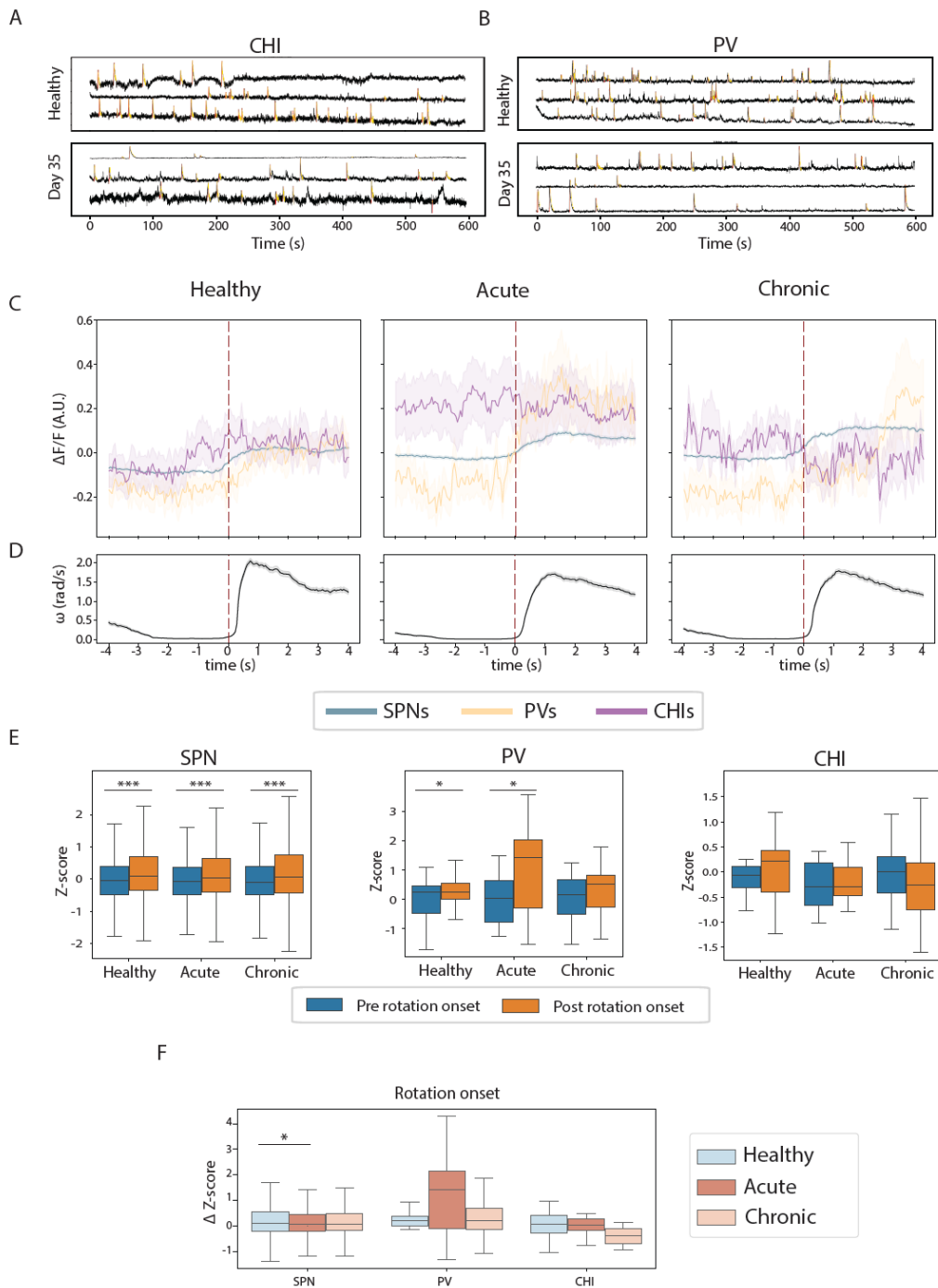
**Figure S3. Population SPN, PV and CHI activity change at rotational onset transitions. Related to Figure 3.**
**(A)** Example GCaMP6 fluorescence traces from CHIs during a session before 6-OHDA injury (top) and on day 35 after 6-OHDA injury (bottom). **(B)** Example GCaMP6 fluorescence traces from PV cells during a session before 6-OHDA injury (top) and on day 35 (bottom) after 6-OHDA injury. **(C)** Population GCaMP6 fluorescence of SPN (blue), PV (yellow), and CHI (purple) aligned to rotational onsets, during healthy (left), acute (middle) and chronic depletion conditions (right). **(D)** Corresponding rotational velocity for the conditions analyzed in **C**. **(E)** Z-scores of mean population GCaMP6 fluorescence for SPN (left), PV (middle) and CHI (right) during 2 second window pre-rotation onset (blue) and post-rotation onset (orange). SPN population activity was elevated at rotation onset under all conditions tested (left). PV population activity was elevated under healthy and acute conditions, but not the chronic condition (middle), whereas CHI population activity was not modulated under any condition. (Two-sided t-tests comparing pre- vs. post-rotation onsets. SPN - Healthy: t=22.58, P=8.85x10$^{-110}$; Acute: t=15.19, P=4.1x10$^{-51}$; Chronic: t=21.87, P= 7.41x10$^{-103}$. PV - Healthy: t = 2.67, P=0.012; Acute: t=2.66, P=0.018; Chronic: t=1.23, P= 0.235. CHI - Healthy: t = 1.12, P=0.28; Acute: t=0.324, P=0.748; Chronic: t=1.51, P=0.145.) **(F)** Change in Z-scores of population fluorescence of SPN, PV and CHI post-rotation onset relative to pre-rotation onset in healthy, acute and chronic depletion conditions. (ANOVA comparing across the 3 conditions. Rotation onset: SPN – F(21736,2)=9.01, P=1.23x10-4; PV – F(66,2) = 2.83, P =0.067; CHI – F(84,2) = 2.13, P = 0.13; Tukey's honest significant difference (HSD) post hoc. SPN: Acute vs. Healthy: P = 0.014; Chronic vs. Healthy: P=0.214).
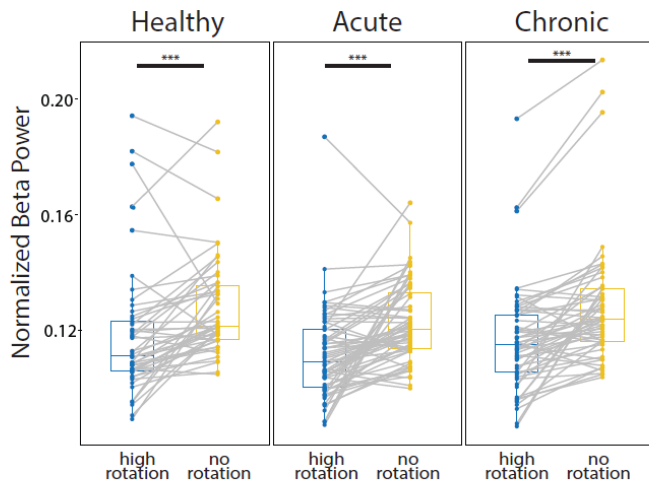
**Figure S4. LFP power was modulated by rotation bouts. Related to Figure 4**

**(A)** LFP power at beta frequency during high-rotation bouts (blue) and no-rotation bouts (yellow), under healthy (left), acute (middle) and chronic depletion conditions (right). Beta power was significantly lower during high-rotation bouts than no-rotation bouts for all three conditions analyzed (Wilcoxon signed-rank. Healthy: $P=7.8\times10^{-6}$; Acute: $P=8.0\times10^{-8}$; Chronic: $P=1.2\times10^{-7}$.) **(B)** Same as **A** but for low-gamma frequencies. High-gamma power was significantly higher during high-rotation bouts than no rotation bouts, for all three conditions analyzed (Wilcoxon signed-rank. Healthy: $P=0.004$; Acute: $P=3.2\times10^{-5}$; Chronic: $P=0.002$.) **(C)** Same as **A** but for high-gamma frequencies. high-gamma power was significantly higher during high-rotation bouts than no rotation bouts, for all three conditions analyzed (Wilcoxon signed-rank. Healthy: $P=3.6\times10^{-4}$; Acute: $P=1.9\times10^{-6}$; Chronic: $P=0.006$.).
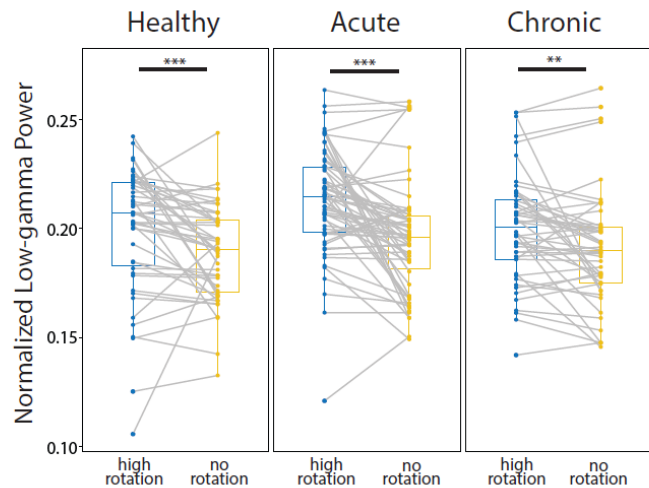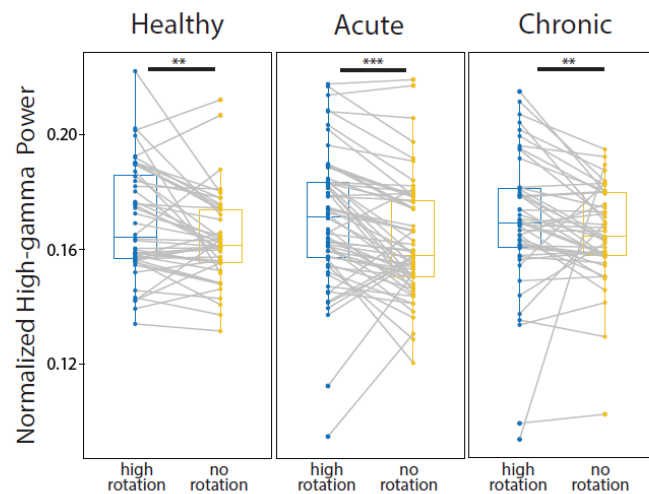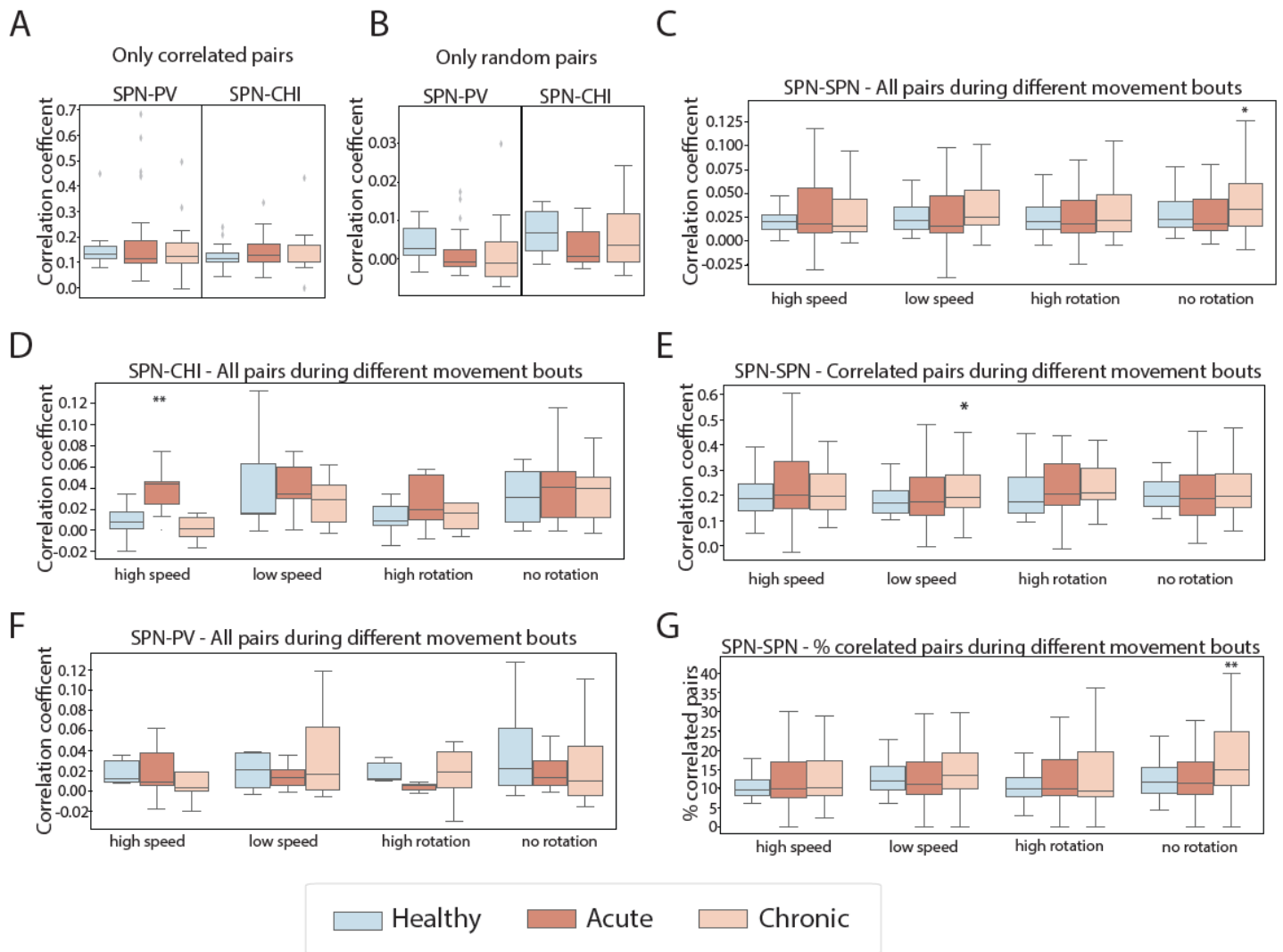
**Figure S5. Pairwise correlation of SPN-SPN, SPN-PV and SPN-CHI during different movement aspects before and after dopamine depletion. Related to Figure 5**

**(A, B)** Correlation coefficients between correlated (**A**) and random (**B**) pairs of SPN-PV (left) and SPN-CHI (right) during healthy (blue), acute (dark orange) and chronic (light orange) conditions. No difference across all conditions (ANOVA for interaction of correlated SPN-PV pairs and conditions: $F_{(2,56)}=0.456$, P=0.637; Random SPN-PV pairs and conditions: $F_{(2,58)}=1.060$, P=0.354; Correlated SPN-CHI pairs and conditions: $F_{(2,41)}=0.126$, P=0.882; random SPN-CHI pairs and conditions: $F_{(2,41)}=1.499$, P=0.2367.) **(C)** Correlation coefficients of all SPN-SPN pairs during high-speed bouts, low-speed bouts, high rotation bouts, and no rotation bouts. There was a significant increase in correlation coefficients for SPN-SPN pairs during the chronic condition (ANOVA for interaction of SPN-SPN correlation in no rotation bouts and conditions: $F_{(2,206)} = 3.550$, P=0.031. Mixed-effect model: Acute vs. Healthy: t=0.436 P=0.663; Chronic vs. Healthy: t=2.343 P=0.020.) **(D)** Correlation coefficients across all SPN-CHI pairs during high-speed bouts, low-speed bouts, high rotation bouts, and no rotation bouts. SPN-CHI correlation coefficients were increased under the acute condition (ANOVA for interaction of SPN-CHI correlation in high-speed bouts and conditions: $F_{(2,28)} = 7.046$, P=0.004. Mixed-effect model: Acute vs. Healthy: t=3.079 P=0.005; Chronic vs. Healthy: t=-0.635 P=0.531.) **(E)** Correlation coefficients of correlated SPN-SPN pairs during various locomotion bouts. There was a significant increase in SPN-SPN correlation coefficients during low-speed bouts under the chronic condition (ANOVA for interaction of SPN-SPN correlations in low-speed bouts and conditions: $F_{(2,197)} = 3.299$, P=0.040. Mixed-effect model: Acute vs. Healthy: t=1.522 P=0.130; Chronic vs. Healthy: t=2.568 P=0.011.) **(F)** Correlation coefficients across all SPN-PV pairs during high-speed bouts, low-speed bouts, high rotation bouts, no rotation bouts. No difference between all comparisons (ANOVA for interaction of SPN-PV correlations during high-speed bouts and conditions: $F_{(2,44)}=0.622$, P=0.542. SPN-PV correlations during low-speed bouts and conditions: $F_{(2,47)}=1.148$, P=0.327. SPN-PV correlations during high-rotation bouts and conditions: $F_{(2,24)}=0.509$, P=0.608. SPN-PV correlations during low-rotation bouts and conditions: $F_{(2,53)}=0.073$, P=0.930.) **(G)** The fraction of correlated SPN-SPN pairs during different locomotion bouts. There was a significant increase in the percentage of correlated SPN-SPN pairs during no rotation bouts (ANOVA for interaction of correlated SPN-SPN pairs in no rotation bouts and conditions: $F_{(2,206)} = 6.336$, P=0.002. Mixed-effect model: Acute vs. Healthy: t=0.047 P=0.963; Chronic vs. Healthy: t=2.831 P=0.005.) All box plots are plotted session wise, with the box representing the median (middle line), 25th (Q1, bottom line) and 75th (Q3, top line), and the whiskers are Q1-1.5*(Q3-Q1) and Q3+1.5*(Q3-Q1).
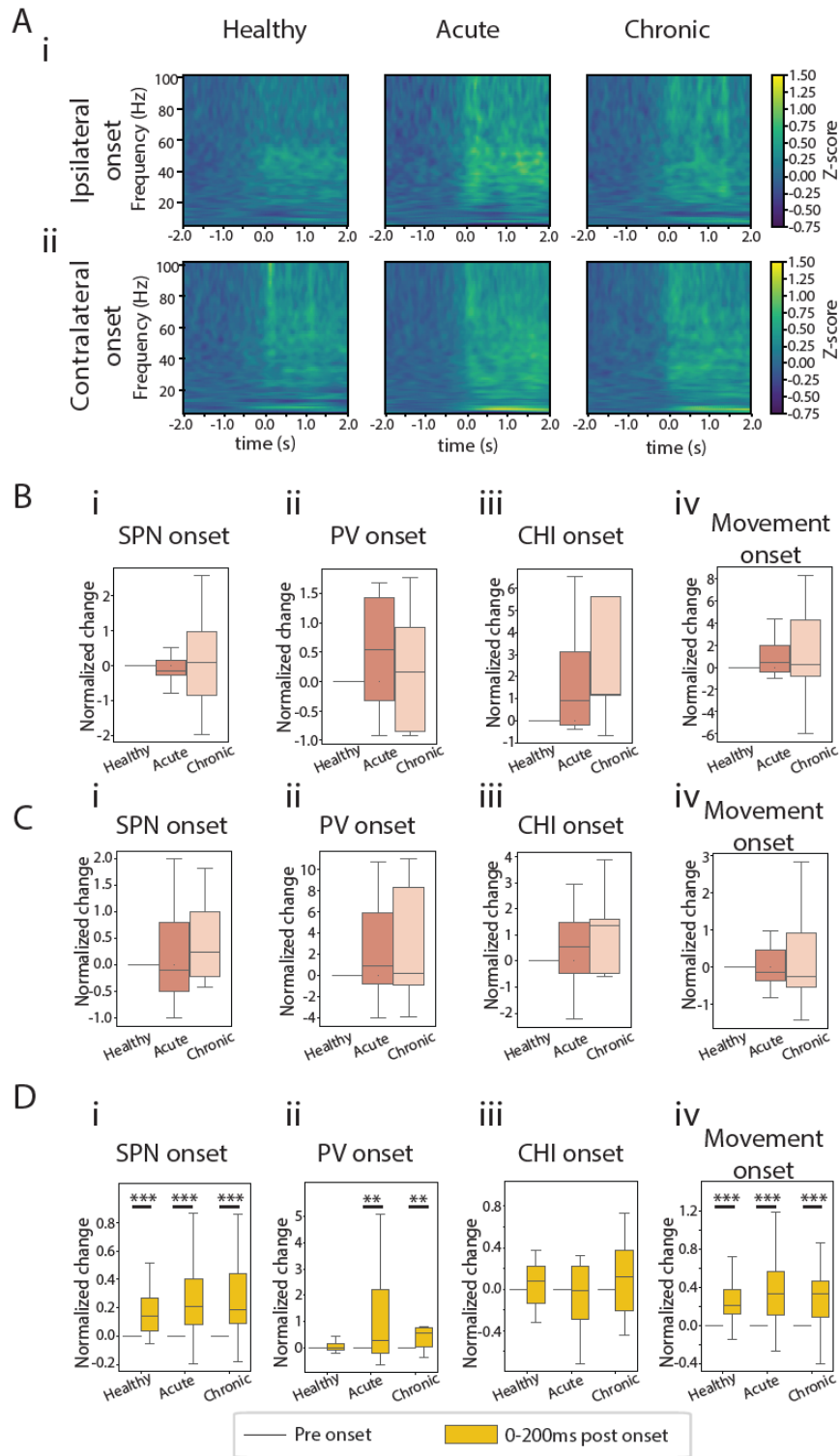
**Figure S6. LFP power following movement onsets or calcium event onsets. Related to Figure 6.**
**(A)** LFP spectrum aligned to ipsilateral rotation onset (**i**) and contralateral rotational onsets (**ii**). **(B)** Beta power change normalized to healthy conditions during the 0-200ms time window following SPN calcium event onset, PV calcium event onset, CHI calcium event onset, and movement onset. No significant differences were found across all conditions. (ANOVA for interaction of beta power after SPN onset and conditions: $F_{(2.209)}=0.814$, $P=0.445$. Beta power after PV onset and conditions: $F_{(2.209)}=0.077$, $P=0.926$; Beta power after CHI onset and conditions: $F_{(2.209)}=1.465$, $P=0.246$.) **(C)** Same as B but for normalized low-gamma power. (ANOVA for interaction of low-gamma power after SPN onset and conditions: $F_{(2.41)}=1.19$, $P=0.312$. Low-gamma power after PV onset and conditions: $F_{(2.15)}=0.609$, $P=0.557$. Low-gamma power after CHI onset and conditions: $F_{(2.13)}=0.928$, $P=0.420$. Low-gamma power after movement onset and conditions: $F_{(2.41)}=0.959$, $P=0.392$.) **(D)** Normalized change in high-gamma power during the 0-200ms windows (yellow) following SPN onset, PV onset, CHI onset, and movement onset compared to pre-onset (black). (Wilcoxon rank test: * $P <0.05$, *** $P < 0.001$.) Boxplots are plotted session wise, with the box representing the median (middle line), 25th (Q1, bottom line) and 75th (Q3, topline), and the whiskers are Q1-1.5*(Q3-Q1), and Q3+1.5*(Q3-Q1).

*Table 1 - Summary of main effects during acute and chronic depletion conditions. Related to Figures 2-6*

| 6-OHDA injury induced changes compared to the healthy condition: | | | Acute | Chronic |
|---|---|---|---|---|
| Behavior (Fig 2) | % time spent in different movement bouts | Low-speed | - | - |
| | | High-speed | - | - |
| | | Contralateral rotation | ↓ | ↓ |
| | | Ipsilateral rotation | - | - |
| | | No rotation | ↑ | ↑ |
| | # of onset transitions | Speed | ↓ | ↓ |
| | | Contralateral rotation | ↓ | ↓ |
| | | Ipsilateral rotation | ↓ | - |
| Calcium activity (Fig. 3, S3) | Event rate | SPN | ↓ | ↓ |
| | | PV | - | - |
| | | CHI | - | - |
| | % cell modulated by speed | SPN | ↓ | - |
| | | PV | - | - |
| | | CHI | - | - |
| | % cell modulated by rotation | SPN | ↓ | - |
| | | PV | ↓ | - |
| | | CHI | - | - |
| | Population changes at movement onset | SPN | ↓ | ↓ |
| | | PV | ↓ | ↓ |
| | | CHI | - | - |
| | Population changes at rotation onset | SPN | ↓ | - |
| | | PV | - | - |
| | | CHI | - | - |
| Correlation (Figs 5, S5) | % correlated pairs | SPN-SPN | - | ↑ |
| | | SPN-PV | - | - |
| | | SPN-CHI | ↑ | - |
| | Overall Pearson correlation coefficient (PCC) | SPN-SPN | - | ↑ |
| | | SPN-PV | - | - |
| | | SPN-CHI | - | - |
| LFP (Fig. 6) | Transient pathological high-gamma power during 200ms post event onset | Speed onset | - | - |
| | | SPN onset | ↑ | ↑ |
| | | PV onset | ↑ | ↑ |
| | | CHI onset | - | - |